

PLATES ON BIPARAMETRIC ELASTIC FOUNDATION BY BDIE METHOD

By J. T. Katsikadelis¹ and L. F. Kallivokas²

ABSTRACT: An efficient boundary differential integral equation (BDIE) method is presented for the analysis of thin elastic plates with free boundaries of any shape resting on biparametric elastic foundation. The plate, which may have holes, is subjected to concentrated loads, line loads, or distributed surface loads. The solution is achieved by converting the governing boundary value problem to an equivalent problem consisting of five coupled boundary equations, two of which are differential and three of which are integral. The boundary differential equations are derived from the boundary conditions, while the boundary integral equations are derived from the integral representations for the deflections of the plate and of the foundation region. A numerical technique based on the discretization of the boundary is developed for the solution of the boundary equations. The computational efficiency of the method is increased by converting the domain integrals attributable to loading into boundary line integrals. Numerical results for several plates are obtained to attest to and demonstrate the accuracy and the efficiency of the presented BDIE method.

INTRODUCTION

The Pasternak-type biparametric elastic foundation model is the most natural extension of the Winkler model for homogeneous soil deposit and the next-highest approximation to the foundation response (Kerr 1964). The biparametric elastic foundation models are derived either as an extension of the Winkler model by imposing interaction between spring elements (Filonenko-Bodorich 1940; Hetenyi 1946; Paternak 1954; Kerr 1964) or by simplifying the three-dimensional continuum (Reissner 1958; Vlasov and Leontiev 1966). Although this foundation model can adequately approximate the soil-structure interaction, an analytical solution to the governing boundary value problem is obtained only when the plate has a simple geometry (e.g. circular plate or rectangular plate). Thus, the use of approximate or numerical methods is inevitable. To this end, the boundary element method can be used efficiently to obtain an accurate solution to the problem. Balaš et al. (1984) have given a boundary integral formulation for the problem at hand and they have obtained results for a circular plate subjected to a centered concentrated force. More recently, Katsikadelis and Kallivokas (1986) have used the boundary element method for plates on a Pasternak-type elastic foundation with a clamped boundary and have obtained numerical results for plates with various shapes, including plates with composite shapes. In this investigation, the

¹Assoc. Prof. of Struct. Analysis, Dept. of Civ. Engrg., Nat. Tech. Univ. of Athens, Zografou Campus, GR-157 73 Athens, Greece.

²Grad. Student, Dept. of Civ. Engrg., Nat. Tech. Univ. of Athens, Athens, Greece.

Note. Discussion open until October 1, 1988. To extend the closing date one month, a written request must be filed with the ASCE Manager of Journals. The manuscript for this paper was submitted for review and possible publication on March 16, 1987. This paper is part of the *Journal of Engineering Mechanics*, Vol. 114, No. 5, May, 1988. ©ASCE, ISSN 0733-9399/88/0005-0847/\$1.00 + \$.15 per page. Paper No. 22454.

plate with free edges resting on a biparametric foundation model is treated. In contrast to the clamped boundary, the free boundary allows interaction between the deflections of the foundation area under the plate and those outside it. Thus, the boundary value problem is much more difficult than that of the clamped plate. The boundary method developed herein is a new one, since it reduces the boundary value problem to an equivalent one involving five coupled boundary equations, two of which are differential and three of which are integral. The differential equations are solved using the finite difference method, while the integral equations are solved using the boundary element method. The presented, which in the following will be referred to as the boundary differential integral equation method (BDIEM), proves to be very efficient. It is worth mentioning that the present formulation avoids hypersingularities in the kernels of the boundary integral equations, since the line integrals are limited to single- or double-layer potentials. This fact facilitates the numerical solution of the boundary integral equations and, thus, from the computational point of view, the proposed method seems to have an advantage over a pure boundary integral equation method. Moreover, in the case of linearly varying loading, the efficiency of the method is improved by converting the domain integral into line integrals on the boundary of the plate. Numerical results are obtained for circular plates, annular plates, rectangular plates, and plates of complex shape. The accuracy of the method is attested to by comparing the results with those existing from analytical or other numerical solutions.

FORMULATION OF THE BOUNDARY VALUE PROBLEM

Consider a thin elastic plate of thickness h , occupying the two-dimensional multiply connected region R of the plate, bounded by the $M + 1$ curves $C_0, C_1, C_2, \dots, C_M$ and resting on a Pasternak-type elastic foundation with subgrade reaction modulus k and shear modulus G . The curves C_i ($i = 0, 1, 2, \dots, M$) may be piecewise smooth; that is, the boundary of the plate may have a finite number of corners (Fig. 1).

Assuming that the plate maintains contact with the subgrade and that there are no friction forces at the interface, its deflection $w(P)$ at any point $P \in R$ satisfies the following differential equation (Kerr 1964):

$$Lw = \frac{f(P)}{D}, \quad P \in R \quad \dots \dots \dots (1)$$

where $f(P)$ = the transverse loading; $D = Eh^3/12(1 - \nu^2)$ = the flexural rigidity of the plate; and L = an operator defined as

$$L = \nabla^4 - \frac{G}{D} \nabla^2 + \frac{k}{D}; \quad \nabla^2 = \frac{\partial^2}{\partial x^2} + \frac{\partial^2}{\partial y^2}; \quad \nabla^4 = (\nabla^2)^2 \quad \dots \dots \dots (2)$$

The interaction pressure p_s between plate and subgrade is given as

$$p_s = kw - G\nabla^2 w \quad \dots \dots \dots (3)$$

If the region exterior to the boundary C_0 is denoted by R_0 while the region inside the boundary curves C_i ($i = 1, 2, \dots, M$) are denoted by R_i ($i = 1, 2, \dots, M$), respectively, the deflection w_F of the subgrade in the

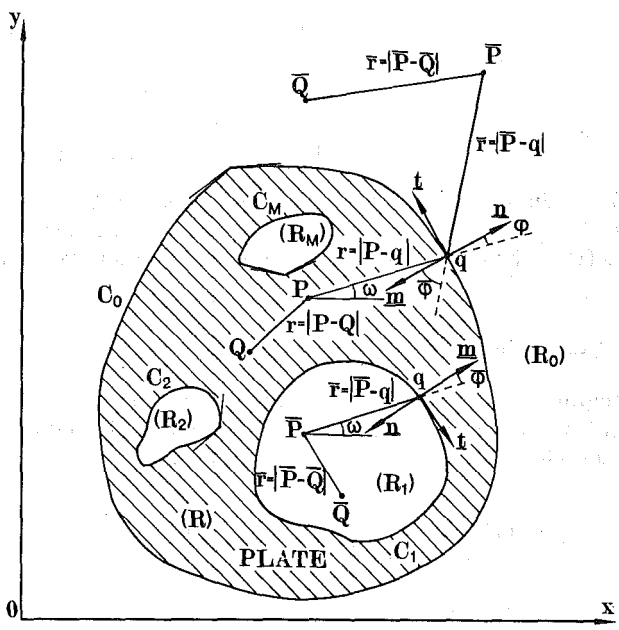


FIG. 1. Two-Dimensional Region of Foundation Area Occupied by Plate

foundation regions R_i ($i = 0, 1, 2, \dots, M$) satisfies the following differential equation:

$$L^* w_F = \frac{g(\bar{P})}{G}, \quad \bar{P} \in R_i \dots \dots \dots (4)$$

where $g(\bar{P})$ = the transverse loading directly applied to the foundation region R_i , and L^* = an operator defined as

$$L^* = \frac{k}{G} - \nabla^2 \dots \dots \dots (5)$$

The boundary conditions for the free boundaries C_i of the plate are derived from the following physical considerations:

1. The deflection is continuous across C_i .
2. The bending moment M_n of the plate vanishes on C_i .
3. The jump of the shear force in the shear layer on C_i , which is due to the discontinuity of slope of the shear layer on the boundary, is equal to the effective shear force of the plate along C_i .

Using intrinsic coordinates (Katsikadelis 1982) the aforementioned conditions in terms of the deflections w of the plate and w_F of the foundation region R_i are expressed as

$$w = w_F \dots \dots \dots (6a)$$

$$-D \left[\nabla^2 w + (\nu - 1) \left(\frac{\partial^2 w}{\partial s^2} + K(s) \frac{\partial w}{\partial n} \right) \right] = 0 \dots\dots\dots (6b)$$

$$-D \left[\frac{\partial}{\partial n} \nabla^2 w - (\nu - 1) \frac{\partial}{\partial s} \left(\frac{\partial^2 w}{\partial s \partial n} - K(s) \frac{\partial w}{\partial s} \right) \right] = G \left(\frac{\partial w_F}{\partial n} - \frac{\partial w}{\partial n} \right) \dots\dots (6c)$$

where $\partial/\partial n$ = the directional derivative along the outward normal to the boundary C_i of the plate; $\partial/\partial s$ = the derivative with respect to the arc length s ; $K(s)$ = the curvature of the boundary; and ν is Poisson's ratio.

INTEGRAL REPRESENTATION OF THE SOLUTION

The integral representation of the solution can be obtained using the Green identity for the operator L and the fundamental solution to Eq. 1.

The Green identity for the self-adjoint operator L is

$$\iint_R (vLw - wLv) d\sigma = \int_C \left(v \frac{\partial}{\partial n} \nabla^2 w - \frac{\partial v}{\partial n} \nabla^2 w - w \frac{\partial}{\partial n} \nabla^2 v + \frac{\partial w}{\partial n} \nabla^2 v - \frac{G}{D} v \frac{\partial w}{\partial n} + \frac{G}{D} w \frac{\partial v}{\partial n} \right) ds \dots\dots\dots (7)$$

where $C = \cup_{i=0}^M C_i$. Eq. 7 is readily obtained by combining the Rayleigh-Green identity for the biharmonic operator (Katsikadelis and Armenakos 1984b) with the classical Green identity for the harmonic operator.

The fundamental solution to Eq. 1 is a singular particular solution of the following differential equation:

$$Lv = \frac{\delta(Q - P)}{D} \dots\dots\dots (8)$$

in which $\delta(Q - P)$ = the Dirac δ -function, Q = the field point; and P = the source point. The nature of the solution to Eq. 8 depends on the quantity $\mu = G^2/4kD$. In this investigation, only the case $\mu < 1$ is considered, and it seems to be valid for usual foundation materials (Kerr 1964). For these values of μ the solution to Eq. 8 is given as (Vlasov and Leontiev 1966)

$$v = v(P, Q) = v(Q, P) = \frac{l^2}{4D \sin 2\theta} \operatorname{Re} [H_0^{(1)}(\beta\rho)] \dots\dots\dots (9)$$

where

$$\rho = \frac{r}{l} \dots\dots\dots (10a)$$

$$l = \sqrt[4]{\frac{D}{k}} \dots\dots\dots (10b)$$

$$\beta = \cos \theta + i \sin \theta \dots\dots\dots (10c)$$

$$2\theta = \arctan \left(-\sqrt{\frac{1}{\mu} - 1} \right) \dots \dots \dots (10d)$$

$r = |P - Q|$ is the distance between the points (P, Q) and $\text{Re}[H_0^{(1)}(\beta\rho)]$ denotes the real part of the zero order Hankel function of the first kind. Notice that when G approaches 0, it can be shown that $v(P, Q)$ reduces to $(-\rho^2/2\pi D)\text{kei}(\rho)$ which is the fundamental solution to the equation governing the plate resting on a Winkler-type elastic foundation (Katsikadelis and Armenakias 1984b).

Applying Eq. 7 for the deflection of the plate w , and the fundamental solution v , which satisfy Eqs. 1 and 8, respectively, and using Eqs. 54a-c Appendix I, the integral representation for the deflection of the plate is obtained as

$$w(P) = \iint_R v(P, Q)f(Q) d\sigma_Q - D \int_C \left[v(P, q)\Psi(q) - \frac{\partial}{\partial n_q} v(P, q)\Phi(q) - \frac{\partial}{\partial n_q} \nabla^2 v(P, q)\Omega(q) + \nabla^2 v(P, q)X(q) - \frac{G}{D} v(P, q)X(q) + \frac{G}{D} \frac{\partial}{\partial n_q} v(P, q)\Omega(q) \right] ds_q \dots \dots \dots (11)$$

or

$$w(P) = \frac{\rho^2}{4 \sin 2\theta} \left\{ F(P) - \int_C [\Lambda_1(\rho_{Pq})\Omega(q) + \Lambda_2(\rho_{Pq})X(q) + \Lambda_3(\rho_{Pq})\Phi(q) + \Lambda_4(\rho_{Pq})\Psi(q)] ds_q \right\} \dots \dots \dots (12)$$

where the following notation has been introduced for conciseness:

$$\Omega(q) = w(q) \dots \dots \dots (13a)$$

$$X(q) = \frac{\partial}{\partial n_q} w(q) \dots \dots \dots (13b)$$

$$\Phi(q) = \nabla^2 w(q) \dots \dots \dots (13c)$$

$$\Psi(q) = \frac{\partial}{\partial n_q} \nabla^2 w(q) \dots \dots \dots (13d)$$

$$F(P) = \frac{1}{D} \iint_R V(\rho_{PQ})f(Q) d\sigma_Q \dots \dots \dots (14)$$

$$\Lambda_1(\rho_{Pq}) = \left[\frac{1}{l} \frac{G}{D} V'(\rho_{Pq}) - \frac{1}{\beta} U'(\rho_{Pq}) \right] \cos \phi \dots \dots \dots (15a)$$

$$\Lambda_2(\rho_{Pq}) = \frac{1}{r^2} U(\rho_{Pq}) - \frac{G}{D} V(\rho_{Pq}) \dots \dots \dots (15b)$$

$$\Lambda_3(\rho_{Pq}) = -\frac{1}{l} V'(\rho_{Pq}) \cos \phi \dots \dots \dots (15c)$$

$$\Lambda_4(\rho_{Pq}) = V(\rho_{Pq}) \dots \dots \dots (15d)$$

$$\rho_{Pq} = \frac{|P - q|}{l} \dots \dots \dots (15e)$$

$$\phi = \mathbf{r}; \mathbf{n} \dots \dots \dots (15f)$$

The functions $V(\rho)$, $V'(\rho)$, $U(\rho)$, $U'(\rho)$ are given by Eqs. 55a-d in Appendix I. In the aforementioned equations, points inside the region R are denoted by upper case letters, while points on the boundary C are denoted by lower case letters. Moreover, the subscripts of the elements $d\sigma$ and ds indicate the point that varies during integration. Furthermore, $\partial/\partial n_q$ denotes the normal derivative taken with respect to point q .

Similarly, using the Green identity for the harmonic operator, the following Green identity is obtained for the operator L^* in the region R_i :

$$\iint_{R_i} (wL^*v - vL^*w) d\sigma = \int_{C_i} \left(v \frac{\partial w}{\partial m} - w \frac{\partial v}{\partial m} \right) ds \dots \dots \dots (16)$$

where $\partial/\partial m$ = the outward normal to the boundary C_i of the region R_i ; that is, $\partial/\partial m = -\partial/\partial n$ (Fig. 1).

The fundamental solution to Eq. 4 is a singular particular solution to the equation

$$L^*u = \frac{\delta(\bar{Q} - \bar{P})}{G} \dots \dots \dots (17)$$

The solution to Eq. 17 (Vlasov and Leontiev 1966) is given as

$$u = u(\bar{P}, \bar{Q}) = u(\bar{Q}, \bar{P}) = \frac{1}{2\pi G} K_0(\bar{\rho}) \dots \dots \dots (18)$$

where

$$\bar{\rho} = \frac{\bar{r}}{l} \dots \dots \dots (19a)$$

$$l = \sqrt{\frac{G}{k}} \dots \dots \dots (19b)$$

$$\bar{r} = |\bar{P} - \bar{Q}| \dots \dots \dots (19c)$$

and $K_0(\bar{\rho})$ = the zero-order modified Bessel function of the second kind.

Applying Eq. 16 for the functions $w = w_F$ and $v = u$, which satisfy Eqs. 4 and 17, respectively, and using the boundary condition of Eq. 6a, the

following integral representation for the deflection $w_F(\bar{P})$, $\bar{P} \in R_i$ ($i = 0, 1, 2, \dots, M$) of the subgrade is obtained:

$$w_F(\bar{P}) = \iint_{R_i} u(\bar{\rho}_{\bar{P}\bar{Q}})g(\bar{Q}) d\sigma_{\bar{Q}} + \int_{C_i} \left[u(\bar{\rho}_{\bar{P}q})\Theta(q) - \frac{\partial}{\partial m_q} u(\bar{\rho}_{\bar{P}q})\Omega(q) \right] ds_q \dots \dots \dots (20)$$

or

$$w_F(\bar{P}) = \frac{1}{2\pi} \left\{ H(\bar{P}) + \int_{C_i} [\Lambda_5(\bar{\rho}_{\bar{P}q})\Theta(q) + \Lambda_6(\bar{\rho}_{\bar{P}q})\Omega(q)] ds_q \right\} \dots \dots \dots (21)$$

where

$$H(\bar{P}) = \frac{1}{G} \iint_{R_i} K_0(\bar{\rho}_{\bar{P}\bar{Q}})g(\bar{Q}) d\sigma_{\bar{Q}} \dots \dots \dots (22)$$

$$\Lambda_5(\bar{\rho}_{\bar{P}q}) = K_0(\bar{\rho}_{\bar{P}q}) \dots \dots \dots (23a)$$

$$\Lambda_6(\bar{\rho}_{\bar{P}q}) = \frac{1}{l} K_1(\bar{\rho}_{\bar{P}q}) \cos \bar{\phi} \dots \dots \dots (23b)$$

$$\Theta(q) = \frac{\partial}{\partial m_q} w_F(q) \dots \dots \dots (24)$$

$$\bar{\rho}_{\bar{P}q} = \frac{|\bar{P} - q|}{l} \dots \dots \dots (25a)$$

$$\bar{\phi} = \bar{\mathbf{r}} \cdot \hat{\mathbf{m}} \dots \dots \dots (25b)$$

$$\hat{\mathbf{m}} = -\mathbf{n} \dots \dots \dots (25c)$$

$K_1(\bar{\rho})$ is the first-order modified Bessel function of the second kind.

DERIVATION OF THE BOUNDARY DIFFERENTIAL AND INTEGRAL EQUATIONS

The loading functions $f(Q)$ and $g(\bar{Q})$ in Eqs. 11 and 20 are given at every point Q in R and \bar{Q} in R_i ($i = 0, 1, 2, \dots, M$), respectively. Moreover, the function $v(P, Q)$ and its derivatives (Eqs. 54 and 55 of Appendix I) as well as the function $u(\bar{P}, \bar{Q})$ (Eq. 18) and its derivative are known. However, the functions $\Omega, X, \Phi, \Psi, \Theta$ are not known on the points of the boundary. These five unknown boundary functions can be established by solving a system of five coupled boundary equations, two of which are differential and three of which are integral.

The boundary differential equations are established from the boundary conditions of Eqs. 6b and 6c, which, by virtue of Eqs. 13a-d and 24, are written as

Downloaded from ascelibrary.org by University of Texas at Austin on 02/15/17. Copyright ASCE. For personal use only; all rights reserved.

$$\Phi + (\nu - 1) \left(\frac{\partial^2 \Omega}{\partial s^2} + KX \right) = 0 \quad (26)$$

$$\Psi - (\nu - 1) \left(\frac{\partial^2 X}{\partial s^2} - \frac{\partial K}{\partial s} \frac{\partial \Omega}{\partial s} - K \frac{\partial^2 \Omega}{\partial s^2} \right) = \frac{G}{D} (\Theta + X) \quad (27)$$

Two boundary integral equations are derived from the integral representation of Eq. 12 using the procedure presented in Katsikadelis and Armenakos (1984a). Thus, by letting point P in Eq. 12 approach a point p on C and by taking into account that in the limiting process the line integral with kernel $\partial \nabla^2 v / \partial n$ exhibits a discontinuity jump equal to

$$\lim_{P \rightarrow p} \int_C \frac{\partial}{\partial n_q} \nabla^2 v(P, q) \Omega(q) ds_q - \int_C \frac{\partial}{\partial n_q} \nabla^2 v(p, q) \Omega(q) ds_q = \frac{1}{2D} \Omega(p) \quad (28)$$

we obtain the first boundary integral equation as

$$\frac{2 \sin 2\theta}{r^2} \Omega(p) + \int_C [\Lambda_1(\rho_{pq}) \Omega(q) + \Lambda_2(\rho_{pq}) X(q) + \Lambda_3(\rho_{pq}) \Phi(q) + \Lambda_4(\rho_{pq}) \Psi(q)] ds_q = F(p) \quad (29)$$

The second integral equation is obtained by applying the operator ∇^2 on both sides of Eq. 12 and subsequently by letting point P approach a point p on the boundary C . Thus, by taking into account that $\nabla^4 v - (G/D) \nabla^2 v = -(k/D)v$ (Eq. 8) and that the line integral with kernel $\partial \nabla^2 v / \partial n$ exhibits a discontinuity jump as $P \rightarrow p \in C$, the second boundary integral equation, which is independent from Eq. 29, is obtained as

$$2 \sin 2\theta \Phi(p) + \int_C [N_1(\rho_{pq}) \Omega(q) + N_2(\rho_{pq}) X(q) + N_3(\rho_{pq}) \Phi(q) + N_4(\rho_{pq}) \Psi(q)] ds_q = G(p) \quad (30)$$

where

$$G(p) = \frac{1}{D} \iint_R U(\rho_{pQ}) f(Q) d\sigma_Q \quad (31)$$

$$N_1(\rho_{pq}) = \frac{1}{r^3} V'(\rho_{pq}) \cos \phi \quad (32a)$$

$$N_2(\rho_{pq}) = -\frac{1}{r^2} V(\rho_{pq}) \quad (32b)$$

$$N_3(\rho_{pq}) = -\frac{1}{r} U'(\rho_{pq}) \cos \phi \quad (32c)$$

$$N_4(\rho_{pq}) = U(\rho_{pq}) \quad (32d)$$

Finally, the third boundary integral equation is derived from Eq. 21 by letting point $\bar{P} \in R_i$ approach a point p on the boundary C_i . Thus, taking into account that the line integral with kernel $\Lambda_6(\bar{p}p_q)$ behaves like a double layer potential (Eq. 57b of Appendix I), the following integral equation is obtained:

$$\pi\Omega(p) - \int_C [\Lambda_5(\bar{p}p_q)\Theta(q) + \Lambda_6(\bar{p}p_q)\Omega(q)] ds_q = H(p) \dots\dots\dots (33)$$

Eq. 33 is valid for all boundaries C_i ($i = 0, 1, 2, \dots, M$). Note that Eqs. 28 and 33 have been derived for points p where the boundary is smooth.

NUMERICAL ANALYSIS

The differential Eqs. 26 and 27 and the integral Eqs. 29, 30, and 33 constitute a set of five simultaneous equations for the unknown boundary functions $\Omega, X, \Phi, \Psi, \Theta$. Elimination of the boundary quantities Ω and Φ would yield three integrodifferential equations, which would complicate the numerical solution of the problem. Of course, integrodifferential equations can be avoided if the integral representation of the solution for the plate is expressed in terms of boundary quantities having direct physical meaning ($w, \partial w/\partial n, M_n, V_n$) (Bezine 1979; Stern 1979; Katsikadelis 1982). However, this approach results in kernels with hypersingularities and, thus, the numerical evaluation of the singular integrals becomes cumbersome, especially in the present case, where the kernels are real and imaginary parts of the Hankel functions with complex argument.

In this section, a straightforward numerical solution of the five coupled boundary equations is developed. The boundary is discretized into a finite number of boundary elements (Fig. 2) and, subsequently, the differential equations are solved using the finite difference method. The integral equations are then solved using the boundary element method with constant element.

Thus, approximating the derivatives by unevenly spaced central finite differences involving the nodal values of Eqs. 26, 27, 29, 30, and 33 are written for the typical point i as

$$(A_{11})_{i,i-1}\Omega_{i-1} + (A_{11})_{i,i}\Omega_i + (A_{11})_{i,i+1}\Omega_{i+1} + (A_{12})_{i,i}X_i + (A_{13})_{i,i}\Phi_i = 0 \dots\dots\dots (34a)$$

$$(A_{21})_{i,i-1}\Omega_{i-1} + (A_{21})_{i,i}\Omega_i + (A_{21})_{i,i+1}\Omega_{i+1} + (A_{22})_{i,i-1}X_{i-1} + (A_{22})_{i,i}X_i + (A_{22})_{i,i+1}X_{i+1} + (A_{24})_{i,i}\Psi_i + (A_{25})_{i,i}\Theta_i = 0 \dots\dots\dots (34b)$$

$$\sum_{j=1}^N [(A_{31})_{ij}\Omega_j + (A_{32})_{ij}X_j + (A_{33})_{ij}\Phi_j + (A_{34})_{ij}\Psi_j] = F_i \dots\dots\dots (34c)$$

$$\sum_{j=1}^N [(A_{41})_{ij}\Omega_j + (A_{42})_{ij}X_j + (A_{43})_{ij}\Phi_j + (A_{44})_{ij}\Psi_j] = G_i \dots\dots\dots (34d)$$

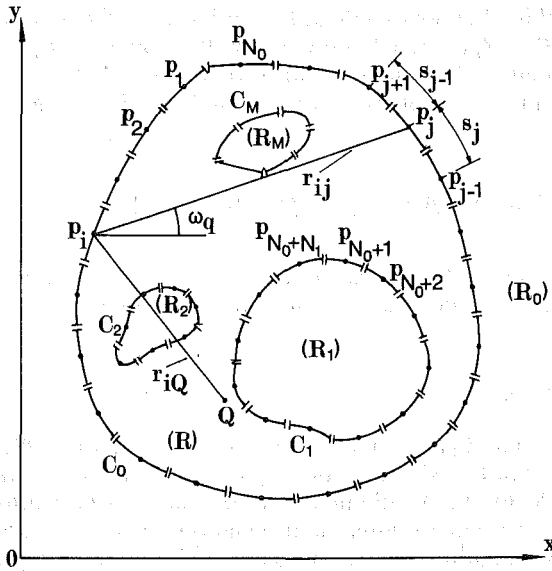


FIG. 2. Discretization of Boundary of Plate

$$\sum_{j=1}^N [(A_{51})_{ij}\Omega_j + (A_{55})_{ij}\Theta_j] = H_i \dots \dots \dots (34e)$$

where $i = 1, 2, \dots, N$; $N =$ the number of boundary elements; and

$$(A_{11})_{i,i-1} = e_i s_i \dots \dots \dots (35a)$$

$$(A_{11})_{i,i} = -e_i (s_i + s_{i-1}) \dots \dots \dots (35b)$$

$$(A_{11})_{i,i+1} = e_i s_{i-1} \dots \dots \dots (35c)$$

$$(A_{12})_{i,i} = 0.5 K_i \dots \dots \dots (35d)$$

$$(A_{13})_{i,i} = \frac{0.5}{(\nu - 1)} \dots \dots \dots (35e)$$

$$(A_{21})_{i,i-1} = \left[2K_i - s_i \left(\frac{\partial K}{\partial s} \right)_i \right] e_i s_i \dots \dots \dots (35f)$$

$$(A_{21})_{i,i} = \left[-2K_i + (s_i - s_{i-1}) \left(\frac{\partial K}{\partial s} \right)_i \right] e_i (s_i + s_{i-1}) \dots \dots \dots (35g)$$

$$(A_{21})_{i,i+1} = \left[2K_i + s_{i-1} \left(\frac{\partial K}{\partial s} \right)_i \right] e_i s_{i-1} \dots \dots \dots (35h)$$

$$(A_{22})_{i,i-1} = -2e_i s_i \dots \dots \dots (35i)$$

$$(A_{22})_{i,i} = 2e_i(s_i + s_{i-1}) - \frac{G}{D(\nu - 1)} \dots \dots \dots (35j)$$

$$(A_{22})_{i,i+1} = -2e_i s_{i-1} \dots \dots \dots (35k)$$

$$(A_{24})_{i,i} = \frac{1}{(\nu - 1)} \dots \dots \dots (35l)$$

$$(A_{25})_{i,i} = -\frac{G}{D(\nu - 1)} \dots \dots \dots (35m)$$

in which $e_i = 1/[s_i s_{i-1} (s_i + s_{i-1})]$; s_{i-1} and s_i are the distances along the boundary between the nodal points $i - 1$, i and i , $i + 1$, respectively (Fig. 2). K_i , $(\partial K/\partial s)_i$ are the values of the curvature and its derivative at point i .

$$(A_{31})_{ij} = \int_j \left[\frac{G}{D} \rho_{iq} V'(\rho_{iq}) - \frac{1}{r^2} \rho_{iq} U'(\rho_{iq}) \right] d\omega_q + \frac{2 \sin 2\theta}{r^2} \delta_{ij} \dots \dots \dots (36a)$$

$$(A_{32})_{ij} = \int_j \left[\frac{1}{r^2} U(\rho_{iq}) - \frac{G}{D} V(\rho_{iq}) \right] ds_q \dots \dots \dots (36b)$$

$$(A_{33})_{ij} = - \int_j \rho_{iq} V'(\rho_{iq}) d\omega_q \dots \dots \dots (36c)$$

$$(A_{34})_{ij} = \int_j V(\rho_{iq}) ds_q \dots \dots \dots (36d)$$

$$(A_{41})_{ij} = \int_j \frac{1}{r^2} \rho_{iq} V'(\rho_{iq}) d\omega_q \dots \dots \dots (36e)$$

$$(A_{42})_{ij} = - \int_j \frac{1}{r^2} V(\rho_{iq}) ds_q \dots \dots \dots (36f)$$

$$(A_{43})_{ij} = - \int_j \rho_{iq} U'(\rho_{iq}) d\omega_q + 2 \sin 2\theta \delta_{ij} \dots \dots \dots (36g)$$

$$(A_{44})_{ij} = \int_j U(\rho_{iq}) ds_q \dots \dots \dots (36h)$$

$$(A_{51})_{ij} = - \int_j \bar{\rho}_{iq} K_1(\bar{\rho}_{iq}) d\omega_q + \pi \delta_{ij} \dots \dots \dots (36i)$$

$$(A_{55})_{ij} = - \int_j K_0(\bar{\rho}_{iq}) ds_q \dots \dots \dots (36j)$$

$\rho_{iq} = |p_i - q|/l$, $\bar{\rho}_{iq} = |p_i - q|/\bar{l}$, p_i is a nodal point, $q \in j$ -element, $\omega_q = \hat{\mathbf{x}}_q$, \mathbf{r}_q and δ_{ij} is the Kronecker-delta. The symbol \int_j indicates integration over the j -element. Notice that in Eqs. 36a, c, e, g, and i the relation $\cos\phi ds = rd\omega$ has been used (Katsikadelis and Armenakos 1984a). Moreover

$$F_i = \frac{1}{D} \iint_R V(\rho_{iq})f(Q) d\sigma_Q \dots\dots\dots (37a)$$

$$G_i = \frac{1}{D} \iint_R U(\rho_{iq})f(Q) d\sigma_Q \dots\dots\dots (37b)$$

$$H_i = \frac{1}{G} \iint_R K_0(\bar{\rho}_{iQ})g(\bar{Q}) d\sigma_{\bar{Q}} \dots\dots\dots (37c)$$

In matrix form Eqs. 34a-e are written as

$$\begin{bmatrix} \mathbf{A}_{11} & \mathbf{A}_{12} & \mathbf{A}_{13} & \mathbf{0} & \mathbf{0} \\ \mathbf{A}_{21} & \mathbf{A}_{22} & \mathbf{0} & \mathbf{A}_{24} & \mathbf{A}_{25} \\ \mathbf{A}_{31} & \mathbf{A}_{32} & \mathbf{A}_{33} & \mathbf{A}_{34} & \mathbf{0} \\ \mathbf{A}_{41} & \mathbf{A}_{42} & \mathbf{A}_{43} & \mathbf{A}_{44} & \mathbf{0} \\ \mathbf{A}_{51} & \mathbf{0} & \mathbf{0} & \mathbf{0} & \mathbf{A}_{55} \end{bmatrix} \begin{bmatrix} \mathbf{\Omega} \\ \mathbf{X} \\ \mathbf{\Phi} \\ \mathbf{\Psi} \\ \mathbf{\Theta} \end{bmatrix} = \begin{bmatrix} \mathbf{0} \\ \mathbf{0} \\ \mathbf{F} \\ \mathbf{G} \\ \mathbf{H} \end{bmatrix} \dots\dots\dots (38)$$

where the elements of the matrices \mathbf{A}_{ij} ($i, j = 1, 2, 3, 4, 5$) are given by Eqs. 35, 36 and

$$\begin{aligned} \mathbf{\Omega}^T &= [\Omega_1 \Omega_2 \Omega_3 \dots \Omega_N]; \mathbf{X}^T = [X_1 X_2 X_3 \dots X_N]; \mathbf{\Phi}^T = [\Phi_1 \Phi_2 \Phi_3 \dots \Phi_N] \\ \mathbf{\Psi}^T &= [\Psi_1 \Psi_2 \Psi_3 \dots \Psi_N]; \mathbf{\Theta}^T = [\Theta_1 \Theta_2 \Theta_3 \dots \Theta_N]; \mathbf{F}^T = [F_1 F_2 F_3 \dots F_N] \\ \mathbf{G}^T &= [G_1 G_2 G_3 \dots G_N]; \mathbf{H}^T = [H_1 H_2 H_3 \dots H_N] \dots\dots\dots (39) \end{aligned}$$

Notice that at corner points the quantity $X = \partial w / \partial n$ is discontinuous and actually the derivative $\partial^2 X / \partial s^2$ cannot be approximated using a central difference scheme. This problem may be treated using backward or forward differences for nodal points before or after the corner, respectively, to approximate the second derivative along the boundary. However, good results have been obtained by ignoring the discontinuity and using small boundary elements near the corners.

Evaluation of Line Integrals in Eqs. 36

When $i \neq j$, the arguments ρ , $\bar{\rho}$ do not vanish and these integrals can be evaluated using any of the known numerical techniques for the evaluation of line integrals. In this investigation, the curved boundary element is approximated by a parabolic arc passing through its nodal and extreme points and its value is computed using eight-point Gaussian quadrature. When $i = j$, the arguments of ρ , $\bar{\rho}$ vanish for $q = p_i$. From Eqs. 56a, e, f, and 57c of Appendix I, it is seen that the line integrals with kernels $V(\rho)$, $\rho V'(\rho)$, $\rho U'(\rho)$, $\bar{\rho} K_1(\bar{\rho})$ are not singular and consequently they are evaluated as in the case $i \neq j$. However, as it is seen from Eqs. 56c and 57a of Appendix I, the line integrals with kernels $U(\rho)$ and $K_0(\bar{\rho})$ have a logarithm-

mic singularity and they are evaluated using the technique presented by Katsikadelis and Armenakias (1985).

Evaluation of Double Integrals in Eqs. 37

We may distinguish the following four cases:

1. The plate is subjected to a concentrated load P at a point Q_0 . In this case, the loading function $f(Q)$ can be represented as

$$f(Q) = P\delta(Q - Q_0) \dots\dots\dots (40)$$

Using Eq. 40 the values of the integrals 37a-b are

$$F_i = \frac{P}{D} V(\rho_{iQ_0}) \dots\dots\dots (41a)$$

$$G_i = \frac{P}{D} U(\rho_{iQ_0}) \dots\dots\dots (41b)$$

where $\rho_{iQ_0} = |p_i - Q_0|/l$.

2. The plate is subjected to a line load $q(s)$ distributed along a curve S^* . In this case the double integrals of Eqs. 37a-b are evaluated using Eqs. 41a-b from the following line integrals along the curve S^* :

$$F_i = \frac{1}{D} \int_{S^*} q(Q) V(\rho_{iQ}) ds_Q \dots\dots\dots (42a)$$

$$G_i = \frac{1}{D} \int_{S^*} q(Q) U(\rho_{iQ}) ds_Q \dots\dots\dots (42b)$$

where $\rho_{iQ} = |p_i - Q|/l, Q \in S^*$.

3. The plate is subjected to a uniform or a linearly varying load $f(Q)$ distributed over an area $R^* \subset R$ of the plate bounded by a curve C^* . In this case, the double integrals of Eqs. 37a-b are converted into the following line integrals on the closed curve C^* (Katsikadelis and Kallivokas 1986):

$$F_i = -\cos 2\theta G_i - \frac{l^2 \sin 2\theta}{D} \left[\epsilon f(p_i) + \int_{C^*} \rho_{iq} I'(\rho_{iq}) f(q) d\omega_q - \int_{C^*} I(\rho_{iq}) \frac{\partial f(q)}{\partial n_q} ds_q \right] \dots\dots\dots (43a)$$

$$G_i = \frac{l^2}{D} \left[\int_{C^*} \rho_{iq} V'(\rho_{iq}) f(q) d\omega_q - \int_{C^*} V(\rho_{iq}) \frac{\partial f(q)}{\partial n_q} ds_q \right] \dots\dots\dots (43b)$$

where $\rho_{iq} = |p_i - q|/l, q \in C^*$; $I(\rho) = Im[H_0^{(1)}(\beta\rho)]$; $\epsilon = -4$ when p_i is inside R^* , $\epsilon = -2$ when p_i is on C^* , and $\epsilon = 0$ when p_i is outside C^* .

Downloaded from ascelibrary.org by University of Texas at Austin on 02/15/17. Copyright ASCE. For personal use only; all rights reserved.

The substitution of the domain integrals by line integrals reduces drastically the required computer time. The line integrals of Eqs. 43a-b, as well as the line integrals of Eqs. 42a-b, are evaluated numerically employing the technique presented by Katsikadelis and Armenàkas (1985). Thus, the curve C^* or S^* is approximated by a finite number of parabolic elements. On each element the line integral is computed and the resulting partial values are summed.

4. In the general case where $f(Q)$ is an arbitrary function, the domain integrals of Eq. 37 can be evaluated using the method presented in (Katsikadelis 1987). Moreover, equations similar to Eqs. 41-43 can also be developed for the numerical evaluation of the double integral in Eq. 37c.

EVALUATION OF THE DEFLECTIONS, STRESS RESULTANTS, AND SUBGRADE REACTIONS

When the matrices A_{ij} ($i, j = 1, 2, 3, 4, 5$), F, G, H are established, the system of simultaneous algebraic Eqs. 38 is solved and the values $\Omega_j, X_j, \Phi_j, \Psi_j, \Theta_j$ of the boundary functions $\Omega(s), X(s), \Phi(s), \Psi(s), \Theta(s)$ at the nodal points are obtained. These values can be used to obtain the deflection, the stress resultants and the subgrade reaction at any point P in the interior of the plate, as well as the deflection of the subgrade outside the plate. Thus, the deflection $w(P)$ is obtained from its integral representation, Eq. 12, while the subgrade reaction is obtained from Eq. 3. For the computation of the double integrals $F(P)$ and $G(P)$ we distinguish again four cases as for the integrals F_i and G_i in previous section. Moreover, the deflection of the subgrade $w_F(P)$, in the region R_i outside the plate, is evaluated from its integral representation, Eq. 21.

The bending moments M_x, M_y , the twisting moment M_{xy} and the shear forces Q_x and Q_y at any point of the plate are given in terms of the deflection (Timoshenko and Woinowsky-Krieger 1959) as

$$M_x = -D \left(\frac{\partial^2 w}{\partial x^2} + \nu \frac{\partial^2 w}{\partial y^2} \right) \dots \dots \dots (44a)$$

$$Q_x = -D \frac{\partial}{\partial x} \nabla^2 w \dots \dots \dots (44b)$$

$$M_y = -D \left(\frac{\partial^2 w}{\partial y^2} + \nu \frac{\partial^2 w}{\partial x^2} \right) \dots \dots \dots (44c)$$

$$Q_y = -D \frac{\partial}{\partial y} \nabla^2 w \dots \dots \dots (44d)$$

$$M_{xy} = -M_{yx} = D(1 - \nu) \frac{\partial^2 w}{\partial x \partial y} \dots \dots \dots (44e)$$

The second and third order derivatives of the deflections in Eqs. 44a-e may be evaluated from the computed values of the deflections with sufficient accuracy using numerical differentiation. However, the accuracy is increased and the computer time is considerably reduced when they are

evaluated by direct differentiation of Eq. 12 using the following combinations of derivatives:

$$d_i = \frac{1}{4 \sin 2\theta} \left[\frac{1}{D} \iint_R B_i(\rho) f \, d\sigma + \frac{1}{l^3} \int_C D_i(\rho) \Omega \, ds + \frac{1}{l^2} \int_C E_i(\rho) X \, ds + \frac{1}{l} \int_C J_i(\rho) \Phi \, ds - \int_C B_i(\rho) \Psi \, ds \right], \quad (i = 1, 2, 3, 4, 5) \dots (45)$$

where

$$d_1 = \frac{\partial^2 w}{\partial x^2} + \frac{\partial^2 w}{\partial y^2} \dots (46a)$$

$$d_2 = \frac{\partial^2 w}{\partial x^2} - \frac{\partial^2 w}{\partial y^2} \dots (46b)$$

$$d_3 = 2 \frac{\partial^2 w}{\partial x \partial y} \dots (46c)$$

$$d_4 = -l \frac{\partial}{\partial x} \nabla^2 w \dots (46d)$$

$$d_5 = -l \frac{\partial}{\partial y} \nabla^2 w \dots (46e)$$

$$B_1(\rho) = U(\rho) \dots (47a)$$

$$B_2(\rho) = C(\rho) \cos 2\omega \dots (47b)$$

$$B_3(\rho) = C(\rho) \sin 2\omega \dots (47c)$$

$$B_4(\rho) = U'(\rho) \cos \omega \dots (47d)$$

$$B_5(\rho) = U'(\rho) \sin \omega \dots (47e)$$

$$D_1(\rho) = -V'(\rho) \cos \phi \dots (48a)$$

$$D_2(\rho) = \left[\frac{2}{\rho} V(\rho) + \frac{4}{\rho^2} U'(\rho) + \frac{8}{\rho^2} \cos 2\theta V'(\rho) \right] \cos (2\omega - \phi) - V'(\rho) \cos 2\omega \cos \phi \dots (48b)$$

$$D_3(\rho) = \left[\frac{2}{\rho} V(\rho) + \frac{4}{\rho^2} U'(\rho) + \frac{8}{\rho^2} \cos 2\theta V'(\rho) \right] \sin (2\omega - \phi) - V'(\rho) \sin 2\omega \cos \phi \dots (48c)$$

$$D_4(\rho) = -U(\rho) \cos \omega \cos \phi + \frac{1}{\rho} V'(\rho) \cos (\omega - \phi) \dots (48d)$$

$$D_5(\rho) = -U(\rho) \sin \omega \cos \phi + \frac{1}{\rho} V'(\rho) \sin (\omega - \phi) \dots \dots \dots (48e)$$

$$E_1(\rho) = V(\rho) \dots \dots \dots (49a)$$

$$E_2(\rho) = \left[V(\rho) + \frac{2}{\rho} U'(\rho) + \frac{4}{\rho} \cos 2\theta V'(\rho) \right] \cos 2\omega \dots \dots \dots (49b)$$

$$E_3(\rho) = \left[V(\rho) + \frac{2}{\rho} U'(\rho) + \frac{4}{\rho} \cos 2\theta V'(\rho) \right] \sin 2\omega \dots \dots \dots (49c)$$

$$E_4(\rho) = V'(\rho) \cos \omega \dots \dots \dots (49d)$$

$$E_5(\rho) = V'(\rho) \sin \omega \dots \dots \dots (49e)$$

$$J_1(\rho) = U'(\rho) \cos \phi \dots \dots \dots (50a)$$

$$J_2(\rho) = U'(\rho) \cos \phi \cos 2\omega - \frac{2}{\rho} C(\rho) \cos (2\omega - \phi) \dots \dots \dots (50b)$$

$$J_3(\rho) = U'(\rho) \cos \phi \sin 2\omega - \frac{2}{\rho} C(\rho) \sin (2\omega - \phi) \dots \dots \dots (50c)$$

$$J_4(\rho) = - \left[\frac{1}{\rho} U'(\rho) \cos (\omega - \phi) + V(\rho) \cos \omega \cos \phi + 2 \cos 2\theta U(\rho) \cos \omega \cos \phi \right] \dots \dots \dots (50d)$$

$$J_5(\rho) = - \left[\frac{1}{\rho} U'(\rho) \sin (\omega - \phi) + V(\rho) \sin \omega \cos \phi + 2 \cos 2\theta U(\rho) \sin \omega \cos \phi \right] \dots \dots \dots (50e)$$

$$C(\rho) = U(\rho) - \frac{2}{\rho} V'(\rho) \dots \dots \dots (51)$$

For an arbitrary loading function $f(Q)$ the double integrals in Eq. 45 may be evaluated using the technique presented in (Katsikadelis 1987). When the loading is due to a concentrated force P at some point Q_0 the double integrals in Eq. 45 can be directly evaluated from equations analogous to Eq. 41. Moreover, when the loading is due to a line load along a curve S^* , the double integrals in Eq. 45 are reduced to line integrals on the curve S^* and they are computed from equations analogous to Eq. 42. Finally, when the plate is loaded by a uniform or a linearly varying load distributed over a region $R^* \subset R$ bounded by a curve C^* the double integrals in Eq. 45 are converted into the following line integrals (Katsikadelis and Kallivokas 1986).

TABLE 1. Deflections, Stress Resultants, and Subgrade Reaction along Radius of Annular Plate ($\nu = 0.3$) Subjected to Uniform Load q and Resting on Biparametric Elastic Foundation ($\lambda = 4, s = 5$)

r/a	w		F_s		M_r		M_θ		Q_r		w_F	
	Boundary differential integral equation method (2)	Analytical solution (3)	Boundary differential integral equation method (4)	Analytical solution (5)	Boundary differential integral equation method (6)	Analytical solution (7)	Boundary differential integral equation method (8)	Analytical solution (9)	Boundary differential integral equation method (10)	Analytical solution (11)	Boundary differential integral equation method (12)	Analytical solution (13)
1.0	0.23838E-02	0.23834E-02	0.54673E+00	0.54715E+00	0.0	0.0	-0.33033E-02	-0.32752E-02	0.67203E-01	0.67084E-01	—	—
1.5	0.35836E-02	0.35837E-02	0.99787E+00	0.99791E+00	0.37433E-02	0.37444E-02	0.44028E-03	0.44060E-03	-0.56005E-02	-0.56085E-02	—	—
2.0	0.37867E-02	0.37867E-02	0.10201E+01	0.10201E+01	0.19784E-02	0.19783E-02	0.65922E-03	0.65922E-03	0.19949E-02	0.19949E-02	—	—
2.5	0.33995E-02	0.33995E-02	0.10023E+01	0.10023E+01	0.48248E-02	0.48246E-02	0.20419E-02	0.20418E-02	0.96512E-02	0.96502E-02	—	—
3.0	0.19256E-02	0.19257E-02	0.51622E+00	0.51618E+00	0.0	0.0	0.12099E-02	0.12068E-02	-0.62407E-01	-0.62423E-01	—	—
0	—	—	—	—	—	—	—	—	—	—	0.41479E-03	0.41470E-03
1/3	—	—	—	—	—	—	—	—	—	—	0.54144E-03	0.54131E-03
2/3	—	—	—	—	—	—	—	—	—	—	0.10392E-02	0.10390E-02
3.5	—	—	—	—	—	—	—	—	—	—	0.36055E-03	0.36056E-03
4.0	—	—	—	—	—	—	—	—	—	—	0.68180E-04	0.68182E-04

Note: r = radial distance; a = inner radius of annular plate.

TABLE 2. Influence Coefficients for Deflections, Stress Resultants, and Subgrade Reaction of Circular Plate ($\nu = 0.3$) Resting on Biparametric Elastic Foundation ($\lambda = 5, \delta = 7$)

(a) Influence coefficients for \bar{w} and \bar{p}_s at $r = 0, \theta = 0$						
Load position θ (1)	Deflection (2)	$\frac{r}{a} = 0$ (3)	$\frac{r}{a} = 0.2$ (4)	$\frac{r}{a} = 0.4$ (5)	$\frac{r}{a} = 0.6$ (6)	$\frac{r}{a} = 0.8$ (7)
0	\bar{w}	0.32073E-02	0.19332E-02	0.89935E-03	0.38850E-03	0.16034E-03
	\bar{p}_s	∞	0.21563E+01	0.35526E+00	0.38010E-01	-0.10929E-01
(b) Influence coefficients for \bar{w} at $r = a, \theta = 0$ and \bar{w}_F at $r = 1, 2a, \theta = 0$						
θ	Deflection	$\frac{r}{a} = 0$	$\frac{r}{a} = 0.2$	$\frac{r}{a} = 0.4$	$\frac{r}{a} = 0.6$	$\frac{r}{a} = 0.8$
0	\bar{w}	0.49027E-04	0.12782E-03	0.33062E-03	0.84935E-03	0.21930E-02
	\bar{w}_F	0.22014E-04	0.56138E-04	0.14068E-03	0.34389E-03	0.80943E-03
$\pi/4$	\bar{w}	0.49027E-04	0.91342E-04	0.14636E-03	0.19038E-03	0.19231E-03
	\bar{w}_F	0.22014E-04	0.40942E-04	0.67892E-04	0.96783E-04	0.10951E-03
$\pi/2$	\bar{w}	0.49027E-04	0.44517E-04	0.33703E-04	0.21910E-04	0.12369E-04
	\bar{w}_F	0.22014E-04	0.20398E-04	0.16335E-04	0.11498E-04	0.71797E-05
$3\pi/4$	\bar{w}	0.49027E-04	0.23755E-04	0.10762E-04	0.46701E-05	0.19309E-05
	\bar{w}_F	0.22014E-04	0.10886E-04	0.50744E-05	0.22725E-05	0.97040E-06
π	\bar{w}	0.49027E-04	0.18671E-04	0.70755E-05	0.26788E-05	0.99849E-06
	\bar{w}_F	0.22014E-04	0.85230E-05	0.32721E-05	0.12521E-05	0.47073E-06
(c) Influence coefficients for $\bar{M}_r, \bar{M}_\phi, \bar{Q}_r, \bar{Q}_\phi$ at $r = 0, \theta = 0$						
θ	Stress resultant	$\frac{r}{a} = 0$	$\frac{r}{a} = 0.2$	$\frac{r}{a} = 0.4$	$\frac{r}{a} = 0.6$	$\frac{r}{a} = 0.8$
0	\bar{M}_r	∞	-0.42820E-02	-0.10623E-01	-0.61353E-02	-0.29011E-02
	\bar{M}_ϕ	∞	0.29433E-01	0.51356E-02	0.70174E-03	-0.47609E-04
	\bar{Q}_r	∞	0.31443E+00	0.21092E-01	-0.97923E-02	-0.81229E-02
	\bar{Q}_ϕ	∞	0.0	0.0	0.0	0.0
$\pi/4$	$\bar{M}_r = \bar{M}_\phi$	∞	0.12575E-01	-0.27438E-02	-0.27168E-02	-0.14743E-02
	$\bar{Q}_r = \bar{Q}_\phi$	∞	0.22233E-00	0.14914E-01	-0.69242E-02	-0.57438E-02

$$\iint_{R^*} f \left(\frac{\partial^2}{\partial x^2} - \frac{\partial^2}{\partial y^2} \right) V(\rho) d\sigma = \frac{1}{l} \int_{C^*} fV'(\rho) \cos(\omega + \phi) ds$$

$$- \int_{C^*} \left[\frac{\partial f}{\partial \xi} \cos(\omega + \phi) - \frac{\partial f}{\partial \eta} \sin(\omega + \phi) \right] V(\rho) ds \dots \dots \dots (52a)$$

$$\iint_{R^*} f \frac{\partial^2}{\partial x \partial y} V(\rho) d\sigma = \frac{1}{l} \int_{C^*} fV'(\rho) \sin \omega \cos(\omega + \phi) ds$$

Downloaded from ascelibrary.org by University of Texas at Austin on 02/15/17. Copyright ASCE. For personal use only; all rights reserved.

TABLE 3. Deflections of Rectangular Plate Resting on Elastic Foundation ($\lambda = 5$, $s = 6$)

x/a (1)	y/b (2)	Boundary differential integral equation method (BDIEM) 68 B.E. (3)	Galerkin's method 16 terms (4)
0.0	0.0	0.159E-02	0.162E-02
0.2	0.0	0.158E-02	0.160E-02
0.4	0.0	0.154E-02	0.154E-02
0.6	0.0	0.143E-02	0.141E-02
0.8	0.0	0.120E-02	0.112E-02
1.0	0.0	0.837E-03	0.670E-03
0.0	0.2	0.159E-02	0.158E-02
0.0	0.4	0.159E-02	0.157E-02
0.0	0.6	0.157E-02	0.161E-02
0.0	0.8	0.142E-02	0.137E-02
0.0	1.0	0.834E-03	0.687E-03

$$- \int_{C^*} \frac{\partial f}{\partial \xi} V(\rho) \sin(\omega + \phi) ds \dots \dots \dots (52b)$$

$$\begin{aligned} \iint_{R^*} f \frac{\partial}{\partial x} \nabla^2 V(\rho) d\sigma &= -\frac{1}{l^2} \int_{C^*} f U(\rho) \cos(\omega + \phi) ds \\ + \frac{1}{l} \int_{C^*} \frac{\partial f}{\partial \xi} V'(\rho) \cos \phi ds &\dots \dots \dots (52c) \end{aligned}$$

$$\begin{aligned} \iint_{R^*} f \frac{\partial}{\partial y} \nabla^2 V(\rho) d\sigma &= -\frac{1}{l^2} \int_{C^*} f U(\rho) \sin(\omega + \phi) ds \\ + \frac{1}{l} \int_{C^*} \frac{\partial f}{\partial \eta} V'(\rho) \cos \phi ds &\dots \dots \dots (52d) \end{aligned}$$

where $x, y \in R$ and $\xi, \eta \in C^*$.

NUMERICAL RESULTS

A computer program has been written for the numerical evaluation of the response of plates with free edges resting on a biparametric elastic foundation by integrating the coupled boundary differential and integral Eqs. 26, 27, 29, 30, and 33 using the numerical technique developed in previous sections. Numerical results have been obtained for circular plates with or without holes, rectangular plates, and plates with complicated shapes subjected to concentrated or uniformly distributed loads. The results are in excellent agreement with those obtained from analytical or other numerical solutions. Notice that for $G = 0$ the solution for the plate resting on a Winkler-type elastic foundation is obtained.

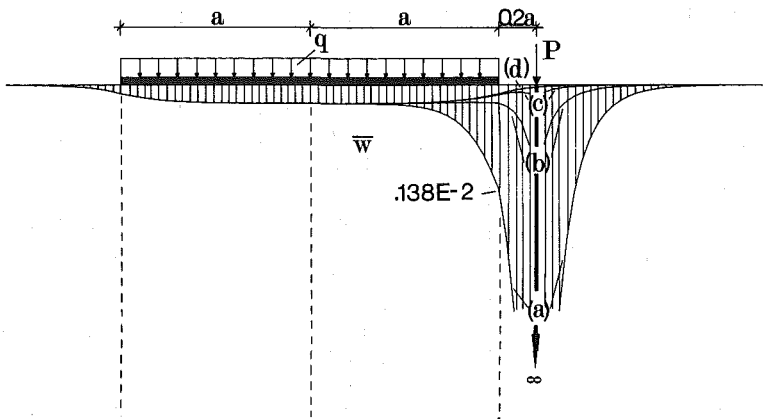


FIG. 3(a). Circular Plate ($\nu = 0.30$) Resting on Elastic Foundation ($\lambda = 8, s = 10$); Curves a, b, c, d for $P = 1, 0.1, 0.01, 0 \pi qa^2$; Deflection $\bar{w} = w/(qa^4/D)$

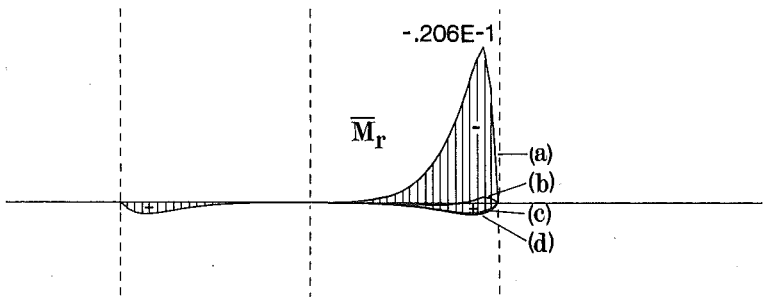


FIG. 3(b). Bending Moment $\bar{M}_r = M_r/qa^2$

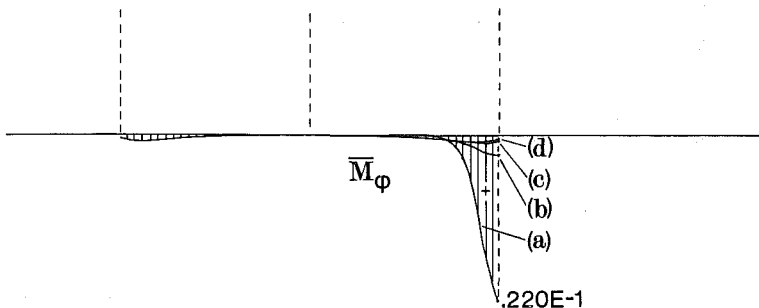


FIG. 3(c). Bending Moment $\bar{M}_\phi = M_\phi/qa^2$

For the presentation of the numerical results, the following dimensionless parameters are used (Katsikadelis and Kallivokas 1986):

$$s = \frac{a}{\sqrt{D/G}} \quad \lambda = \frac{a}{\sqrt{D/k}} \quad \dots \quad (53)$$

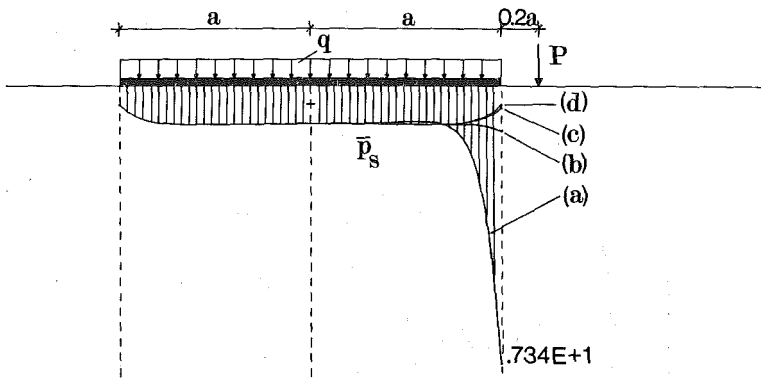


FIG. 3(d). Subgrade Reaction $\bar{P}_s = P_s/q$

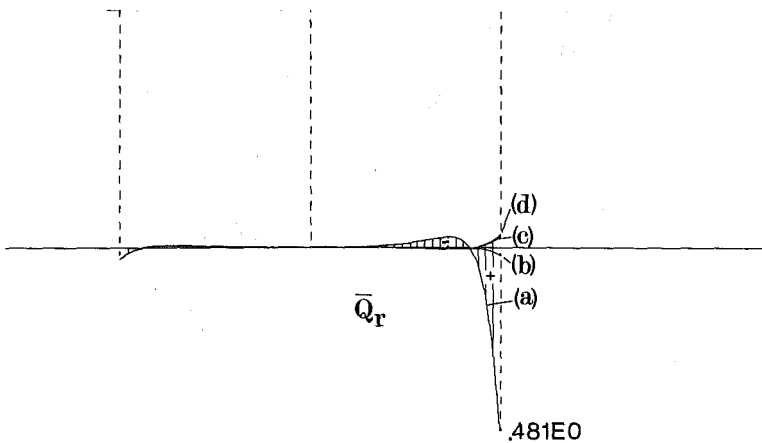


FIG. 3(e). Shear Force $\bar{Q}_r = Q_r/qa$

where a = a characteristic length of the plate (e.g. the radius of a circular plate, the length of one side of a rectangular plate, etc.). The shear modulus G may vary from 0–40 MN/m, while the subgrade reaction modulus k may vary from 0–200 MN/m³. Thus, for usual engineering applications it is $0 \leq s \leq 30$ and $0 \leq \lambda \leq 20$.

To check the accuracy of the proposed BDIE method, a circular and an annular plate have been analyzed. The numerical results are in excellent agreement with those obtained from analytical solutions (Selvadurai 1979). The deflections $\bar{w} = w/(qa^4/D)$, $\bar{w}_F = w_F/(qa^4/D)$, the stress resultants $\bar{M}_r = M_r/qa^2$, $\bar{M}_\phi = M_\phi/qa^2$, $\bar{Q}_r = Q_r/qa$ and the subgrade reaction $\bar{p}_s = p_s/q$ for the annular plate ($\nu = 0.3$) with radii a and $3a$, subjected to a uniform load q and resting on a biparametric elastic foundation ($\lambda = 4$, $s = 5$) are presented in Table 1. The results have been obtained using 48 boundary elements (32 for the external and 16 for the internal boundary). It is apparent that relatively few boundary elements are sufficient to obtain accurate results.

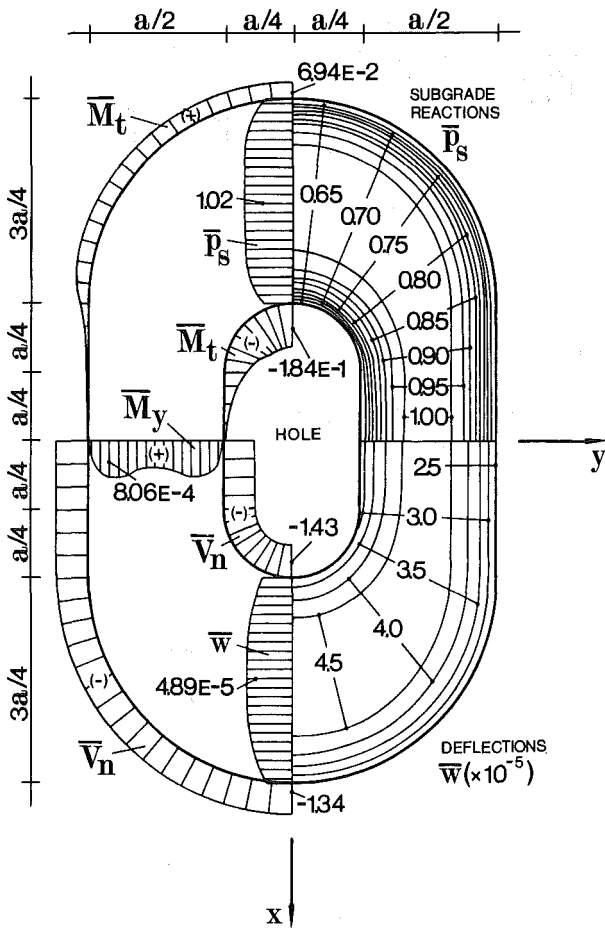


FIG. 4. Plate of Composite Shape on Elastic Foundation ($\lambda = 12, s = 10$)

In Table 2, the influence coefficients for the deflection $\bar{w} = w/(Pa^2/D)$, the stress resultants $\bar{M}_r = M_r/P$, $\bar{M}_\phi = M_\phi/P$, $\bar{Q}_r = Q_r a/P$, $\bar{Q}_\phi = Q_\phi a/P$ and the subgrade reaction $\bar{p}_s = p_s a^2/P$ at point $r = 0, \theta = 0$ as well as for the deflection $\bar{w}_F = w_F/(Pa^2/D)$ at point $r = 1.2a, \theta = 0$ of a circular plate with free edge for various positions of the concentrated load P are presented ($\lambda = 5, s = 7, \nu = 0.3$). The results have been obtained using 32 boundary elements.

In Table 3 numerical results for a rectangular plate ($\nu = 0.3, 2a \times 2b, b/a = 2$) resting on an elastic foundation ($\lambda = 5, s = 6$) and subjected to a uniform load q are presented as compared with those obtained using the approximate Galerkin method was sixteen terms (Vlasov and Leontiev 1966).

In Figs. 3(a)–3(e) the influence of a concentrated load, applied at a point outside a circular plate ($\nu = 0.3, \lambda = 8, s = 10$), on the deflections, stress resultants, and subgrade reactions along the diameter through the load P is

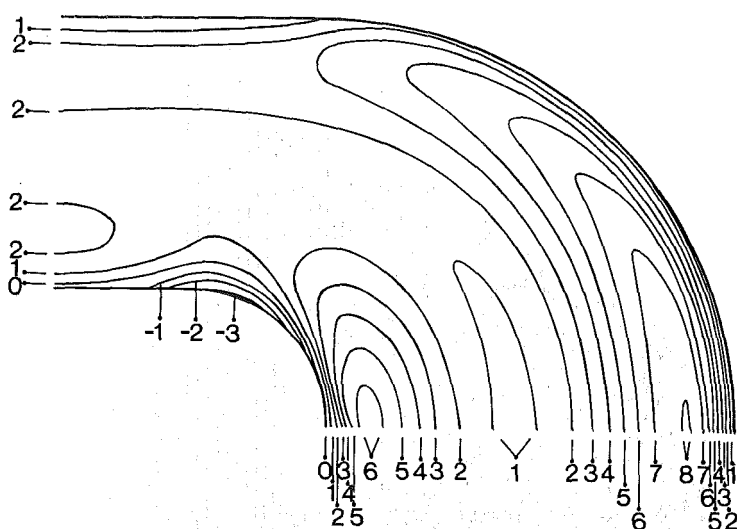


FIG. 5. Contour Plot of Bending Moment $\bar{M}_x = M_x/qa^2$ (Magnification Factor 10^4)

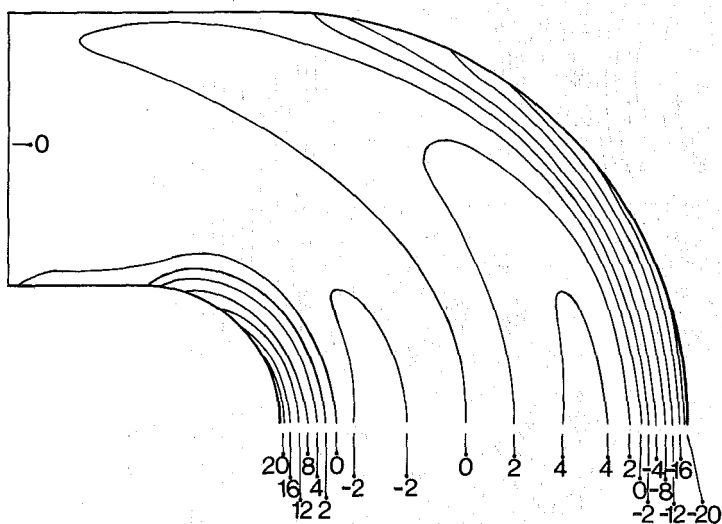


FIG. 6. Contour Plot of Shearing Forces $\bar{Q}_x = Q_x/qa$ (Magnification Factor 10^3)

presented. The plate is subjected to a uniform load. The results have been obtained using 32 boundary elements.

Finally, a plate of composite shape ($\nu = 0.30$) with free boundaries resting on an elastic foundation ($\lambda = 12, s = 10$) and subjected to a uniform load q has been analyzed. The results obtained on the basis of BDIEM using 68 boundary elements are presented in Figs. 4-7. More specifically, in Fig. 4 the distributions of the boundary reaction $\bar{V}_n = V_n/qa$ and bending

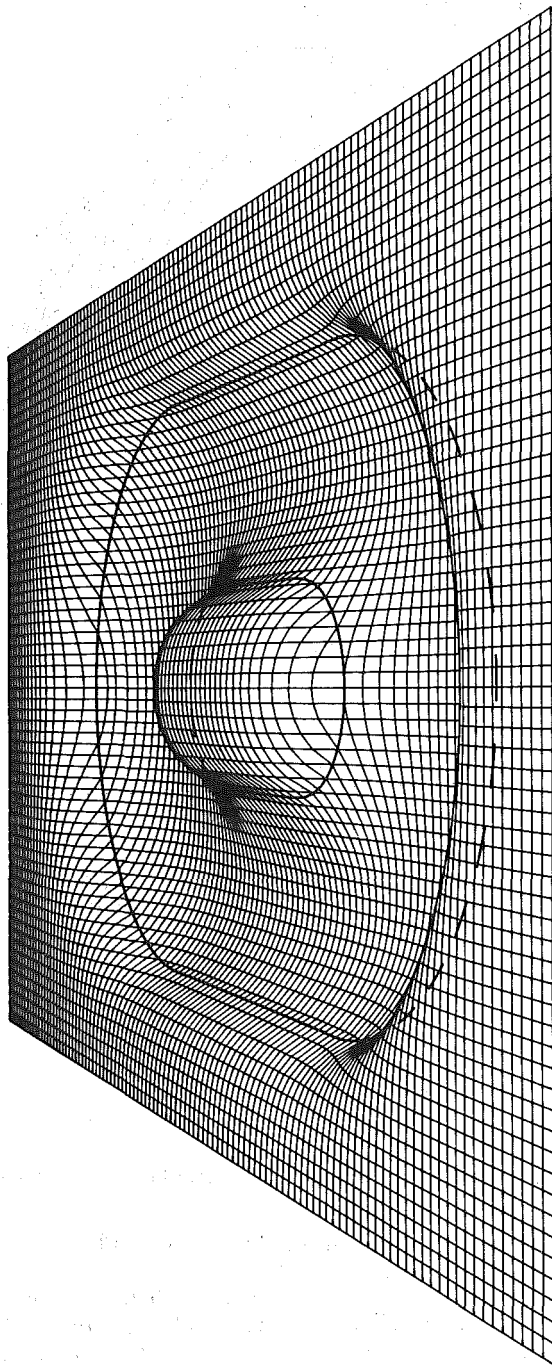


FIG. 7. Perspective of Deflection Surface of Plate and Surrounding Foundation Region

moments $\bar{M}_x = M_x/qa^2$, $\bar{M}_y = M_y/qa^2$ as well as the distributions and contour plots of the deflection $\bar{w} = w/(qa^4/D)$ and subgrade reaction $\bar{p}_s = p_s/q$ are presented. In Figs. 5 and 6 the contour plots of the bending moment $\bar{M}_x = M_x/qa^2$ and shearing force $\bar{Q}_x = Q_x/qa$ of the plate are shown. These results are considered accurate because they differ negligibly from those obtained using twice as many boundary elements.

CONCLUDING REMARKS

In this investigation, a boundary equation method is developed to analyze plates with free edges resting on a Pasternak-type biparametric elastic foundation and subjected to any kind of loading. The worked-out examples show that the presented method is efficient in treating plates with complicated shape, also including holes. The interaction between the plate and the loading in the foundation area outside the plate is also encountered. The method is well-suited for computer-aided analysis. The computation of the line integrals is simplified, since the present formulation avoids hypersingular kernels. Moreover, the conversion of the domain integrals into line integrals reduces the computation time considerably. The present approach renders the boundary equation method a powerful tool to solve difficult plate problems involving complicated boundary conditions.

ACKNOWLEDGMENTS

The numerical results have been partly obtained using the computer of the Hellenic Army EDP Center. The authors are grateful to the Ministry of National Defense. Thanks are also due to the Director of the Center Vice-Colonel P. Galatas and to the system analyst D. Pantelopoulos for their cooperation and kind assistance.

APPENDIX I. FUNCTIONS $V(\rho)$, $V'(\rho)$, $U(\rho)$, AND $U'(\rho)$

In this Appendix certain functions are introduced which are useful for the evaluation of the derivatives of the fundamental solutions of Eqs. 9 and 18.

From Eq. 9 we obtain

$$\frac{\partial v}{\partial n} = \frac{l}{4D \sin 2\theta} V'(\rho) \cos \phi \dots \dots \dots (54a)$$

$$\nabla^2 v = \frac{1}{4D \sin 2\theta} U(\rho) \dots \dots \dots (54b)$$

$$\frac{\partial}{\partial n} \nabla^2 v = \frac{1}{4lD \sin 2\theta} U'(\rho) \cos \phi \dots \dots \dots (54c)$$

in which ()' denotes differentiation with respect to the argument ρ ; $\phi =$ the angle between \mathbf{r} and \mathbf{n} (Fig. 1); and

$$V(\rho) = \text{Re} [H_0^{(1)}(\beta\rho)] \dots \dots \dots (55a)$$

$$V'(\rho) = \text{Re} [-\beta H_1^{(1)}(\beta\rho)] = -\cos \theta \text{Re} [H_1^{(1)}(\beta\rho)] + \sin \theta \text{Im} [H_1^{(1)}(\beta\rho)] \dots \dots \dots (55b)$$

$$U(\rho) = \text{Re} [-\beta^2 H_0^{(1)}(\beta\rho)] = -\cos 2\theta \text{Re} [H_0^{(1)}(\beta\rho)] + \sin 2\theta \text{Im} [H_0^{(1)}(\beta\rho)] \dots \dots \dots (55c)$$

$$U'(\rho) = \text{Re} [\beta^3 H_1^{(1)}(\beta\rho)] = \cos 3\theta \text{Re} [H_1^{(1)}(\beta\rho)] - \sin 3\theta \text{Im} [H_1^{(1)}(\beta\rho)] \dots \dots \dots (55d)$$

The real valued functions $\text{Re}[H_0^{(1)}(\beta\rho)]$, $\text{Im}[H_0^{(1)}(\beta\rho)]$, $\text{Re}[H_1^{(1)}(\beta\rho)]$, $\text{Im}[H_1^{(1)}(\beta\rho)]$ involved in the foregoing relations denote the real and imaginary part of the Hankel functions $H_0^{(1)}(\beta\rho)$, $H_1^{(1)}(\beta\rho)$ and they are evaluated from their series expressions which are given by Zinke (1959).

From the series expressions of the functions $V(\rho)$, $V'(\rho)$, $U(\rho)$ and $U'(\rho)$ we find that

$$\lim_{\rho \rightarrow 0} V(\rho) = 1 - \frac{2\theta}{\pi} \dots \dots \dots (56a)$$

$$\lim_{\rho \rightarrow 0} V'(\rho) = 0 \dots \dots \dots (56b)$$

$$\lim_{\rho \rightarrow 0} U(\rho) \sim \ln \rho \dots \dots \dots (56c)$$

$$\lim_{\rho \rightarrow 0} U'(\rho) \sim \frac{1}{\rho} \dots \dots \dots (56d)$$

$$\lim_{\rho \rightarrow 0} [\rho V'(\rho)] = 0 \dots \dots \dots (56e)$$

$$\lim_{\rho \rightarrow 0} [\rho U'(\rho)] = \frac{2 \sin 2\theta}{\pi} \dots \dots \dots (56f)$$

Moreover, for the modified Bessel functions $K_0(\bar{\rho})$ and $K_1(\bar{\rho})$ it is valid (Abramowitz and Stegun 1972):

$$\lim_{\bar{\rho} \rightarrow 0} K_0(\bar{\rho}) \sim \ln \bar{\rho} \dots \dots \dots (57a)$$

$$\lim_{\bar{\rho} \rightarrow 0} K_1(\bar{\rho}) \sim \frac{1}{\bar{\rho}} \dots \dots \dots (57b)$$

$$\lim_{\bar{\rho} \rightarrow 0} \bar{\rho} K_1(\bar{\rho}) = 1 \dots \dots \dots (57c)$$

APPENDIX II. REFERENCES

- Handbook of mathematical functions (1972). Abramowitz, M., and Stegun, I., eds., 10th Ed., Dover, New York, N.Y., 355-389.
- Balaš, J., Sládek, V., and Sládek, J. (1984). "The boundary integral equation method for plates resting on a two parameter foundation." *Zeitschrift für Angewandte Mathematik und Mechanik*, 64(3), 137-146.
- Bezine, G. P. (1978). "Boundary integral formulation for plate flexure with arbitrary boundary conditions." *Mech. Res. Commun.*, 5(4), 197-206.
- Filonenko-Borodich, M. M. (1940). "Some approximate theories of the elastic foundation." *Uchenye Zapiski Moskovskogo Gosudarstvennogo Universiteta, Mekhanika* (Scientific Notes of the Moscow State University, Mechanics), 46, 3-18 (in Russian).
- Hetyenyi, M. (1946). Beams on elastic foundation. The University of Michigan Press, Ann Arbor, Mich.
- Katsikadelis, J. T. (1982). "The analysis of plates on elastic foundation by the boundary integral equation method," Thesis presented to the Polytechnic Institute of New York at New York, N.Y., in partial fulfillment of the requirements for the degree of Doctor of Philosophy.
- Katsikadelis, J. T. (1987). "A Gaussian quadrature technique for two-dimensional domains of arbitrary shape." to be published.
- Katsikadelis, J. T., and Armenakias, A. E. (1984a). "Analysis of clamped plates on elastic foundation by the boundary integral equation method." *J. Appl. Mech.*, 51(Sept.), 574-580.
- Katsikadelis, J. T., and Armenakias, A. E. (1984b). "Plates on elastic foundation by BIE method." *J. Engrg. Mech.*, ASCE, 110(7), 1086-1105.
- Katsikadelis, J. T., and Armenakias, A. E. (1985). "Numerical evaluation of line integrals with a logarithmic singularity." *J. Amer. Inst. Aeronautics and Astronautics*, 23(7), 1135-1137.
- Katsikadelis, J. T., and Kallivokas, L. F. (1986). "Clamped plates on Pasternak-type elastic foundation by the boundary element methods." *J. Appl. Mech.*, 108(Dec.), 909-917.
- Kerr, A. D. (1964). "Elastic and viscoelastic foundation models." *J. Appl. Mech.*, 31(Sept.), 491-498.
- Pasternak, P. L. (1954). "On a new method of analysis of an elastic foundation by means of two foundation constants." *Gosudarstvennoe Izdatelstvo Literaturi po Stroitelstvu i Arkhitekture*, (State Publications on Construction Literature, Architecture), Moscow, USSR (in Russian).
- Reissner, E. (1958). "A note on deflection of plates on viscoelastic foundation." *J. Appl. Mech.*, 25(Mar.), 144-145.
- Selvadurai, A. P. S. (1979). *Elastic analysis of soil-foundation interaction*. Elsevier, New York, N.Y.
- Stern, M. (1979). "A general boundary integral formulation for the numerical solution of plate bending problems." *Int. J. of Solids and Structures*, 15(10), 769-782.
- Timoshenko, S., and Woinowsky-Krieger, S. (1959). *Theory of plates and shells*. 2nd Ed., McGraw-Hill, New York, N.Y.
- Vlasov, V. Z., and Leontiev, N. N. (1966). *Beams, plates and shells on elastic foundations*. Israel Program for Scientific Translations, Jerusalem, Israel, 161-183.
- Zinke, O. (1959). *Elementare Einführung in die Bessel-Neumann-und Hankel-Funktionen*. S. Hirzel Verlag, Stuttgart, W. Germany, 31-33 (in German).

APPENDIX III. NOTATION

The following symbols are used in this paper:

- C_0 = external boundary of plate (Fig. 1);
 C_1, \dots, C_M = internal boundaries of plate (Fig. 1);

- $D = Eh^3/12(1 - \nu^2)$ = flexural rigidity of plate;
 E = modulus of elasticity of plate;
 $f(P)$ = loading function of plate;
 $F(P)$ = function defined by Eq. 14;
 $g(P)$ = loading function of foundation region;
 G = foundation shear modulus;
 $G(P)$ = function defined by Eq. 31;
 h = thickness of plate;
 $H(\bar{P})$ = function defined by Eq. 22;
 $I(\rho), I'(\rho)$ = kernel functions defined in Appendix I;
 k = foundation reaction modulus;
 $K(s)$ = curvature of boundary;
 l = parameter having dimensions of length defined by Eq. (10b);
 \bar{l} = parameter having dimensions of length defined by Eq. (19b);
 L = differential operator defined by Eq. 2;
 L^* = differential operator defined by Eq. 5;
 \mathbf{n} = direction vector of outward normal to boundary of plate;
 p, q = points on boundary of plate;
 P, Q = points inside region R of plate;
 \bar{P}, \bar{Q} = points in foundation region outside plate;
 p_s = interaction pressure between plate and subgrade;
 r = distance between any two points of plate;
 \bar{r} = distance between any two points in foundation region outside plate;
 R = region occupied by plate (Fig. 1);
 R_0 = foundation region outside C_0 (Fig. 1);
 R_1, \dots, R_M = foundation regions inside boundary curves C_1, \dots, C_M (Fig. 1);
 s = dimensionless parameter defined by Eq. 53;
 $u(\bar{P}, \bar{Q})$ = fundamental solution to Eq. 18;
 $U(\rho), U'(\rho)$ = kernel functions defined in Appendix I;
 $v(P, Q)$ = fundamental solution to Eq. 9;
 $V(\rho), V'(\rho)$ = kernel functions defined in Appendix I;
 w = deflection of plate;
 w_F = deflection of subgrade in foundation area outside plate;
 β = complex parameter defined by Eq. 10c;
 θ = angle defined by Eq. 10d;
 Θ_i = value of $\partial w_F / \partial m$ on i -th boundary element;
 λ = dimensionless parameter defined by Eq. 53;
 $\Lambda_i(\rho)$ = kernel functions defined by Eqs. 15 and 23;
 μ = $G^2/4kD$ parameter characterizing behavior of fundamental solution;
 ν = Poisson's ratio;
 $N_i(\rho)$ = kernel functions defined by Eqs. 32;
 $\rho = r/l$ = dimensionless distance between any two points of plate;

- $\bar{\rho} = \bar{r}/l =$ dimensionless distance between any two points in foundation region outside plate;
 $\varphi =$ angle shown in Fig. 1;
 $\bar{\varphi} =$ angle shown in Fig. 1;
 $\Phi_i =$ value of $\nabla^2 w$ on i -th boundary element;
 $X_i =$ value of $\partial w/\partial n$ on i -th boundary element;
 $\Psi_i =$ value of $\partial(\nabla^2 w)/\partial n$ on i -th boundary element;
 $\omega =$ angle between directions \mathbf{x} and \mathbf{r} (Fig. 1); and
 $\Omega_i =$ value of w on i -th boundary element.